Involvement of a tissue-specific autoantibody in skin disorders of murine systemic lupus erythematosus and autoinflammatory diseases

Hiroyuki Nishimura*† and Jack L. Strominger†

Department of Molecular and Cellular Biology, Harvard University, 7 Divinity Avenue, Cambridge, MA 02138

Contributed by Jack L. Strominger, December 13, 2005

Human systemic lupus erythematosus (SLE) and its murine model, MRL *lpr*/*lpr* mice, are well known to develop a wide range of symptoms, such as glomerulonephritis, dermatitis, and arthritis, as an immune-complex disease. However, the deposition of circulating immune complex does not fully explain the tissue specificity of disease. Tissue-specific autoantigens may also be involved in tissue inflammation. In this study, desmoglein 3 (Dsg3), a major component of epidermal desmosomes, was identified as a skin-specific autoantigen. Several murine models of skin inflammation were found to develop autoantibodies to Dsg3 tightly correlated with disease aggravation, especially in MRL *lpr*/*lpr* mice. Furthermore, SLE-prone skin disease-free FcγRIIb-deficient mice developed skin inflammation upon immunization with Dsg3. Taken together with histological studies, we concluded that skin-specific Dsg3 serves as an autoantigen in chronic skin inflammatory diseases accompanied by mast cell degranulation, including both murine SLE and other autoinflammatory diseases.

autoimmunity | desmoglein 3 | mutant mice

Humans with systemic lupus erythematous (SLE), a prototypic autoimmune disease, develop a wide range of manifestations, such as glomerulonephritis, arthritis, and dermatitis (1). These tissue damages have been thought to be caused by immune-complex deposition in the respective tissues or organs. Indeed, affected glomeruli in kidney as well as dermal–epidermal junctions in skin lesions (2) contain Ig depositions. However, whether or not a tissue-specific autoantigen that participates in disease development is present has not been studied, although non-tissue-specific anti-dsDNA and anti-ribonucleoprotein antibodies have been extensively examined (3).

Several well studied mouse strains provide models of human SLE:MRL-Mp Tnfrsf6^{lpr} (MRL *lpr*/*lpr*) (4), NZB/W F1 (5) and BXSB/*Yaa* (6). Among these murine models, MRL *lpr*/*lpr* mice have the unique characteristic that skin inflammation occurs spontaneously at high frequency. The skin disease, consisting of epidermal thickening and increased cellularity of inflammatory cells in the dermis along with collagen deposition, is different from that seen in human cutaneous SLE (2). However, to obtain a clue for understanding human cutaneous SLE, this model is still very valuable because of the lack of other appropriate murine models. Genetic studies with MRL *lpr*/*lpr* mice clearly demonstrated that B lymphocytes are required for skin disease (7). Moreover, decay-accelerating factor (CD55) deficiency aggravated skin inflammation in MRL *lpr*/*lpr* mice, suggesting the involvement of a complement (8). Considering that skin-disease-free NZB/W F1 mice have Ig deposition at the dermal–epidermal junction (9) that is not sufficient for skin inflammation, skin-specific autoantibodies may play a role in exacerbating or amplifying the skin disease manifestation.

Recently, several reviews have been published about the pathomechanisms of autoinflammatory diseases (sterile autoimmunity or innate autoimmunity). Components of the innate immune system, such as macrophages and neutrophils, play important roles in their pathogenesis without a requirement for lymphoid cells that are important in autoimmune diseases (10–12). In mice, flaky (fsn) (13, 14) and viable motheaten (me^v) (15) can be categorized as autoinflammatory diseases in which skin inflammation occurs without a requirement of T or B lymphocytes (16, 17). In contrast, MRL *lpr*/*lpr* mice, the murine SLE model, develop skin inflammation with a requirement of T and B lymphocytes, which histologically resembles that seen in autoinflammatory disorders. These disorders may have common pathomechanisms despite the different requirements for lymphoid cells. Indeed, both autoinflammatory (myeloid) and autoimmune (lymphoid) components may be present in many or most disorders of self-attack, with the proportions differing widely in different diseases and at different disease phases.

In this paper, desmoglein 3 (Dsg3) (18), a member of the cadherin superfamily, was identified as a tissue-specific autoantigen in MRL *lpr*/*lpr* mice, and anti-Dsg3 IgA was found to be most correlated with skin disease aggravation. In addition, anti-Dsg3 was also found in other skin autoinflammatory disorders, the histology of which resembles that of MRL *lpr*/*lpr* mice. Moreover, a recombinant Dsg3 (rDsg3) protein could induce skin inflammation in FcγRIIb-deficient mice. The possible role of Dsg3 as a tissue-specific autoantigen will be discussed.

Results

Identification of Dsg3 as a Tissue-Specific Autoantigen in MRL *lpr*/*lpr* Mice. MRL *lpr*/*lpr* mice, a representative murine model of an immune-complex disease, were examined so that we could learn more about tissue-specific autoantigens. We also examined three other mouse strains that have skin inflammation that is genetically determined and occurs spontaneously: fsn (13, 14) and me^v (15) mice as autoinflammatory diseases in which skin inflammation occurs without requirement of T or B lymphocytes (16, 17) and scurfy mice as an autoimmune T cell-mediated skin disease (19, 20). Sera from MRL *lpr*/*lpr* mice (from five of seven mice) reacted to a 110-kDa protein in 1% Triton X-100 whole-skin extract by Western blotting (Fig. 1 *Left*). Judging from the molecular size, this protein was thought to be Dsg3 (18), a member of the cadherin superfamily known as a major desmosomal component in epidermis and oral mucosa. To test this hypothesis, whole extract of skin from Dsg3-deficient mice (21) was first examined; the corresponding 110-kDa band was not detected with the sera. For further confirmation, the sera were found to react with the truncated extracellular region of mouse

Conflict of interest statement: No conflicts declared.

Abbreviations: SLE, systemic lupus erythematosus; Dsg3, desmoglein 3; rDsg3, recombinant Dsg3; CGG, chicken γ-globulin; me^v, viable motheaten; fsn, flaky; PV, pemphigus vulgaris; HRP, horseradish peroxidase.

*Present address: Department of Molecular Immunology, Institute of Advanced Medicine, Wakayama Medical University, 811-1 Kimiidera, Wakayama 641-0012, Japan.

†To whom correspondence may be addressed: E-mail: nishimur@wakayama-med.ac.jp or jlstrom@fas.harvard.edu.

www.pnas.org/cgi/doi/10.1073/pnas.0510756103

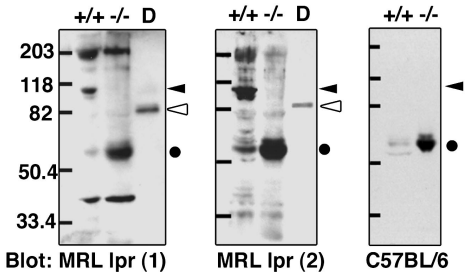

Fig. 1. Dsg3 detected with sera from MRL *lpr*/*lpr* mice. Whole-skin extract (100 μg) from wild type (+/+) and Dsg3-deficient (−/−) mice were subjected to Western blotting with the indicated sera: Seven sera from 5- to 6-month-old MRL *lpr*/*lpr* (MRL *lpr*) and two from 6-month-old C57BL/6 mice were tested. Representative pictures are shown. MRL *lpr*(1) and MRL *lpr*(2) are sera from different individuals. D indicates a lane with 100 ng of mouse rDsg3 (open arrowhead). Filled arrowheads indicate the size of a protein recognized by sera from five of seven MRL *lpr*/*lpr* mice. Filled dots indicate IgH recognized by goat anti-mouse IgG (second antibody, data not shown). The numbers on the left indicate molecular sizes in kDa. All of the whole-extract-transferred membranes were checked by ponceau S staining to ensure equivalent loading of skin extracts.

rDsg3 (22). To further confirm the tissue specificity of Dsg3, Western blot was performed with whole extracts from different tissues of wild-type mice. In liver, spleen, and muscle cell extracts, 35-, 110-, and 200-kDa bands, respectively, were found as major and common bands that were reactive with sera from MRL *lpr*/*lpr* mice (from four of four mice). To ask whether these proteins, especially the 110-kDa protein from spleen, were related to Dsg3, the respective tissue extracts from Dsg3-deficient mice were examined; all three bands were detected with the sera; thus, they were not related to Dsg3 (data not shown). Sera from me^{v} mice (from three of three mice) also reacted with the 110-kDa band present in skin extract from wild-type but not from Dsg3-deficient mice. This band was not detected by sera from fsn, scurfy, or wild-type C57BL/6 mice (Fig. 1 *Right* and data not shown).

Time Course of Appearance of Anti-Dsg3 Antibodies in MRL *lpr*/*lpr* Mice. To further investigate autoantibodies to Dsg3 (anti-Dsg3) semiquantatively and to examine the relationship between anti-Dsg3 and the skin disease course, ELISA, a test with higher sensitivity, was performed with human rDsg3 (22). The relative intensity of anti-Dsg3 in sera from MRL *lpr*/*lpr* mice was significantly increased from as early as 2 months of age to 6 months, as compared with those from 12-month-old control C57BL/6 mice (Fig. 2*A Left* and *Center*). Interestingly, sera from fsn mice at 13 weeks of age, when skin inflammation was in full bloom, also showed significant reactivity to Dsg3 by ELISA (Fig. 2*A Right*, lane 1) as compared with those from control BALB/cBy and A/J (Fig. 2*A Right*, lanes 2 and 3; $P < 0.05$, $n = 6$), although anti-Dsg3 was not detected by Western blot. Consistent with the data from Western blot, sera from me^{v} mice had higher reactivity to Dsg3 than fsn sera ($P < 0.05$) (Fig. 2*A Right*, compare lanes 4 and 1). One of four sera from scurfy mice had reactivity to Dsg3 (Fig. 2*A Right*, lane 5), but there was no statistically significant difference with those from control C57BL/6 mice (Fig. 2*A Right*, lane 6). Next we checked whether other autoimmune strains that do not develop skin inflammation had anti-Dsg3 (data not shown). NZB/W F1 background, another SLE strain, had a slight tendency to increased anti-Dsg3, but the titers even at the age of 10 months never reached those of 13-week-old fsn mice. The homozygous *lpr* mutation also resulted in a relatively low increase of anti-Dsg3 in both C57BL/6 and C3H backgrounds. The titers of sera from these two strains at ages 8–12 months finally reached the level of that

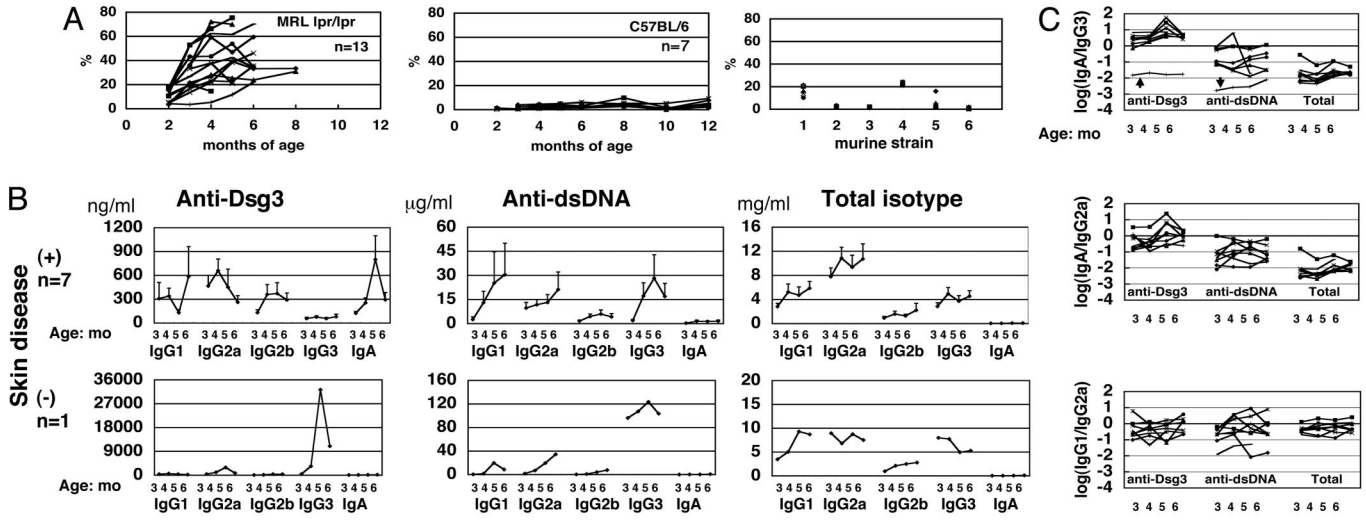

Fig. 2. Time course of appearance of anti-Dsg3, anti-dsDNA, total isotypes, and skin inflammation. (*A*) Sera from MRL *lpr*/*lpr* (*Left*) ($n = 13$) and C57BL/6 (*Center*) ($n = 7$) at the indicated age were examined by ELISA for relative intensity (%) of anti-Dsg3. All mice were observed from 2–3 months to 12 months of age. Values from each individual mouse are connected with lines that are discontinued at the death of that mouse. (*Right*) Sera from several murine models of skin inflammation were tested: strain 1, six fsn at the age of 14 weeks; strain 2, six BALB/By at 14 weeks; strain 3, two A/J at 14 weeks; strain 4, four me^{v} at 8 weeks; strain 5, four scurfy at 4 weeks; and strain 6, four C57BL/6 at 8 weeks. Relative intensity (%) was determined by the following formula: (values from sera)/(a value obtained by binding of HRP-conjugated anti-E tag to coated E-tagged rDsg3) × 100. In some cases, values for individual mice overlapped. (*B*) Isotypes of anti-Dsg3 (*Left*), anti-dsDNA (*Center*), and total amount of isotypes (*Right*) were determined with sera from seven skin-diseased MRL *lpr*/*lpr* mice (*Upper*) and one non-skin-diseased mice (*Lower*) at the indicated months of age. The values are expressed as means ± SEM in *Upper*. (*C*) The logarithms of the ratios of two isotypes of anti-Dsg3 or anti-dsDNA and total isotype amount in *B* were calculated to examine the correlation and specificity between the logarithmic values and skin inflammation. Of 10 combinatorial profiles, 3 are shown and the remaining 7 are not shown. In the logarithm of anti-Dsg3 IgA/IgG3, a sharp peak was present at the age of 5 months, and a cluster of these values had little overlap with those of anti-dsDNA or total isotypes, whereas the other logarithmic profiles had significant overlaps. Values from each individual mouse are connected with lines. Arrows in *Top* indicate the values from the single non-skin-diseased MRL *lpr*/*lpr* mouse; arrows are not shown in *Middle* and *Bottom*, where these values were buried in the clusters of values.

in sera from fsn mice at 13 weeks. NOD mice, a model of type I diabetes, developed no anti-Dsg3.

Isotypic Analysis of Anti-Dsg3 Antibodies in MRL *lpr*/*lpr* Mice. Because no tight correlation was present in MRL *lpr*/*lpr* mice between the appearance of anti-Dsg3 and skin inflammation, which develops at an average age of 4 months, the Ig isotypes of anti-Dsg3 were then examined by ELISA along with anti-dsDNA isotypes and total isotypes as controls. Eight MRL *lpr*/*lpr* mice were examined, of which seven at the average age of 4 months developed skin inflammation, which then expanded. Anti-Dsg3 IgA was increased from 4 to 5 months of age (Fig. 2*B Upper*) and was highly correlated with skin inflammation aggravation, whereas the other isotypes of anti-Dsg3 generally decreased. The titer of anti-Dsg IgA then sharply decreased (Fig. 2*B*). The time at which the titer of each isotype of anti-Dsg3 changed was not correlated to that of anti-dsDNA or total isotypes, suggesting the uniqueness of the Dsg3 autoantibodies. Because of high individual variance of the isotype titer of anti-Dsg3, the individual mouse profiles were reexamined (data not shown). Six of the seven MRL *lpr*/*lpr* mice showed appearance and increase of anti-Dsg3 IgA after macroscopic skin inflammation occurred and increased in size, whereas the other isotypes generally decreased, confirming the significance of anti-Dsg3 IgA. Interestingly, one MRL *lpr*/*lpr* mouse that did not show any evidence of skin disease had much higher anti-Dsg3 IgG3, anti-dsDNA IgG3, and total IgG3, suggesting a possible protective role of IgG3 in skin inflammation (Fig. 2*B Lower*). To devise a more accurate formula that showed correlation of isotypes of anti-Dsg3 and skin inflammation and that integrated the importance of IgA and IgG3 isotypes of anti-Dsg3, the logarithms of the ratios of two isotypes of anti-Dsg3 were calculated. Of ten combinatorial profiles (Fig. 2*C* and data not shown), the logarithm of IgA over IgG3 was found to show the most reliable correlation with skin inflammation (Fig. 2*C Top*); the values from the seven skin-diseased mice showed sharp peaks at the age of 5 months, and this group of values was sharply separated from that of the single nondiseased mouse (arrow). These values were also separated from those of anti-dsDNA and total isotypes, although less sharply (Fig. 2*C Top*). In the logarithms of the ratios of the other combinations of isotypes, the values of anti-Dsg3 generally overlapped with or were inseparable from those of anti-dsDNA and total isotypes (Fig. 2*C Middle* and *Bottom* and data not shown). Thus, the increase of anti-Dsg IgA was most correlated with the aggravation of skin inflammation. Sera from the other mouse strains above were also examined for isotypes of anti-Dsg3, but no definite conclusion could be reached because of their lower titers of anti-Dsg3 and the limitation of ELISA sensitivity.

Induction of Skin Disease in FcγRIIB-Deficient Mice by Immunization of Dsg3. To investigate whether Dsg3 is responsible for skin inflammation, an unsuccessful attempt was first made to affect the skin inflammation in severity and time of onset by immunization with rDsg3 or by injection of i.v. Ig (which was found to contain human anti-Dsg3 at a concentration of 100 ng/ml, data not shown). Next, C57BL/6 FcγRIIb-deficient mice that spontaneously develop SLE-like glomerulonephritis but not skin inflammation (23, 24) and little, if any, anti-Dsg3 (data not shown) were used. These mice also develop arthritis and a Goodpasture syndrome-like disease by immunization with collagen types II and IV, respectively (25, 26). Eight of 10 C57BL/6 FcγRIIb-deficient mice immunized with rDsg3 displayed skin lesions, such as vesicles and pustules, eventually with erosion and hair loss in tails and/or paws or mammary areas and solitary ulcers on the back, whereas only one of 11 C57BL/6 FcγRIIb-deficient mice immunized with control NP-chicken γ-globulin (NP-CGG) developed a solitary ulcer on the back (Fig. 3 *A1–A5* and Table 1). None of control C57BL/6 mice immunized with rDsg3 or NP-CGG developed any sign of skin disease. Upon histological examination, epidermal thickening and extensive edema beneath epidermis were present in some lesions along with massive infiltration of inflammatory cells on tail lesions (Fig. 3 *B2* compared with control in *B1*). Neutrophils also infiltrated into thickened epidermis, generating microabscesses

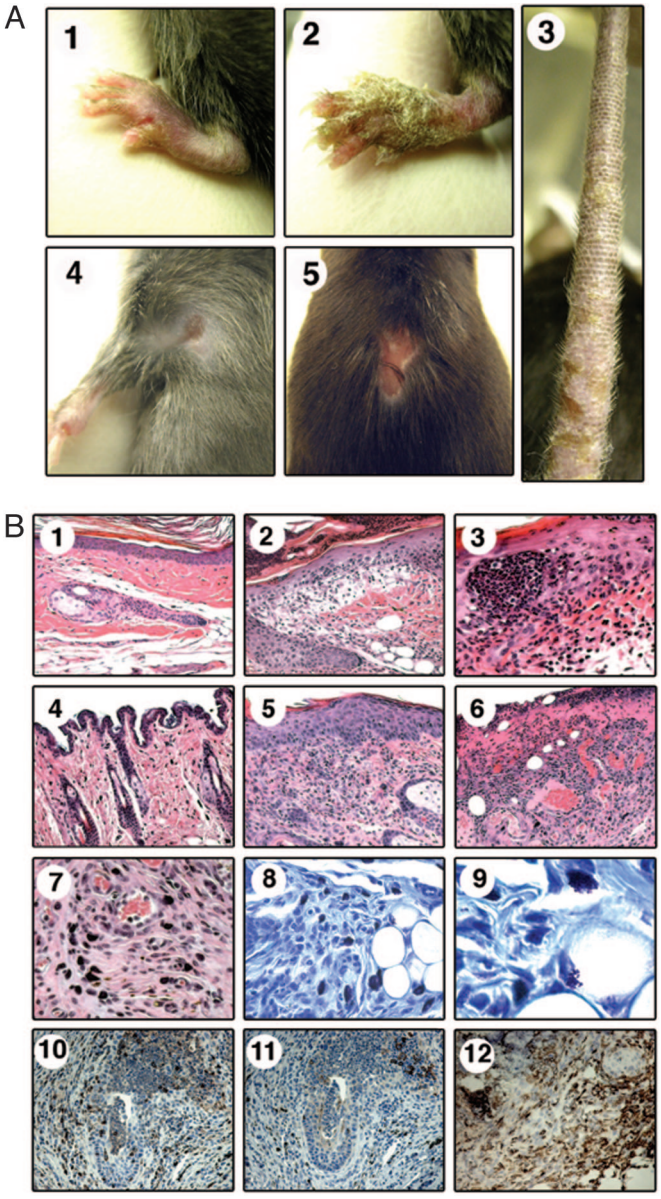

Fig. 3. Macroscopic, histological, and immunohistological analysis of skin inflammation in C57BL/6-FcγRIIb-deficient mice immunized with rDsg3. (*A1* and *A2*) FcγRIIb-deficient mice immunized with rDsg3 developed tiny erosions on the paw (*A1*), which generally expanded into scab formation on the entire paw (*A2*). (*A3*) Some mice developed tiny vesicles, pustules, and erosion on the tail. (*A4* and *A5*) Erosions also occurred in the skin on the mammary gland (*A4*), and a solitary ulcer occurred on the back (*A5*). (*B1–B12*) Skin tissues were from C57BL/6 mice (*B1* and *B4*) and C57BL/6-FcγRIIB-deficient mice (*B2*, *B3*, and *B5–B12*) immunized with human rDsg3. Representative stainings are shown from tails (*B1–B3*) or back skin (*B4–B12*). (*B1–B7*) Hematoxylin/eosin staining. (*B8* and *B9*) Toluidine blue and methylene green staining. (*B10–B12*) Sections were stained with mouse anti-CD3 (*B10*), anti-B220 (*B11*), and anti-F4/80 (*B12*) (brown-stained cells), followed by counterstaining with hematoxylin. (Magnifications: *B1*, *B2*, *B4–B6*, and *B10–B12*, ×80; *B3*, *B7*, and *B8*, ×160; and *B9*, ×504.)

Table 1. Summary of rDsg3 immunization

Mouse strain/ antigen	Total mice examined, *n*	Pustules/vesicles and tiny alopecia in tail, *n* (%)	Pustules/vesicles and tiny alopecia in tail and paws, *n* (%)	Erosion/ulcer in bakc, *n* (%)	Death w/o obvious skin lesions, *n* (%)	Healthy, *n* (%)
B6FcγRIIB/Dsg3	10	1 (10)	3 (30)	4 (40)	1 (10)	1 (10)
B6FcγRIIB/CGG	11	0	0	1 (9)	1 (9)	9 (82)
B6/Dsg3	6	0	0	1 (16)	1 (16)	5 (84)
B6/CGG	6	0	0	0	0	6 (100)

Indicated number of FcγRIIb-deficient and control B6 mice in total were immunized with Dsg3 or control NP-CGG (CGG). Three different patterns of skin lesions were observed as indicated.

(Fig. 3*B3*). On back lesions, epidermal thickening and ulceration in some areas were also seen (Fig. 3 *B5* and *B6* in comparison with control *B4*). In the dermis, massive inflammatory cell infiltration and dilated vessels were seen (Fig. 3 *B5* and *B6*). From immunohistological studies, the inflammatory cells were composed mostly of F4/80-positive myeloid cells and of T and B cells [Fig. 3 *B10* (CD3), *B11* (B220), and *B12* (F4/80)]. Interestingly, an increased number of dark, large cells was found in this severe skin inflammation (Fig. 3*B7*). Toluidine blue and methylene green staining clearly showed that these large cells were mast cells having granules in their cytoplasm with metachromasie (Fig. 3 *B8* and *B9*). In addition, deposited granules were also found (Fig. 3*B9*).

Common Histological Features in Skin Disease Accompanied by Anti-Dsg3. Next the skin inflammation of MRL *lpr/lpr*, fsn, me^v, and scurfy mice was reexamined to seek a common feature of skin inflammation correlating with involvement of Dsg3 as an autoantigen. Epidermal thickening was found in MRL *lpr/lpr*, fsn, and scurfy mice with inflammation in the dermis but not in me^v mice that had inflammation in the deep dermis to s.c. tissues (data not shown and Table 2). Thus, thickening was correlated with the site of inflammation. When toluidine blue and methylene green staining was performed, an increased number of mast cells was found in the dermis of MRL *lpr/lpr* and fsn mice, and in the deep dermis to s.c. tissue of me^v mice (data not shown). In addition, at higher magnification, degranulation of mast cells was also confirmed in all three of these mice (data not shown). On the contrary, skin inflammation in scurfy mice had no mast cell infiltration, although massive inflammation occurred. Rather, epitheloid cells, a macrophage derivative, were present, suggesting a T cell-mediated chronic delayed hypersensitivity reaction. Furthermore, no mast cells were present either in glomerulonephritis of MRL *lpr/lpr* mice or in insulitis of islets in NOD mice (data not shown).

Discussion

By Western blotting with sera from MRL *lpr/lpr* mice, an immune-complex disease in which the roles of tissue-specific autoantigens and autoantibodies in disease development have not been well studied, four tissue-specific autoantigens were found: 110 kDa in skin, 35 kDa in liver, 110 kDa in spleen, and 200 kDa in muscle. Among these autoantigens, the 110-kDa protein in skin was proven to be a desmosomal component Dsg3, a member of the cadherin superfamily. Indeed, anti-Dsg3 developed in MRL *lpr/lpr* mice, and an increase in anti-Dsg3 IgA was most correlated with the aggravation of skin disease. In addition, anti-Dsg3 was also increased in the two fsn and me^v autoinflammatory skin models, although to a lesser degree, whereas the T cell-mediated scurfy skin inflammation barely had anti-Dsg3 (Table 2). Moreover, immunization with rDsg3 induced skin inflammation in C57BL/6 FcγRIIb-deficient mice. Thus, Dsg3 serves as a tissue-specific autoantigen in several skin inflammatory disorders, besides human bullous pemphigus vulgaris (PV) (see below).

Histological pictures of skin inflammation disorders and arthritic lesions in immune-complex diseases as well as autoinflammatory diseases are, in general, called nonspecific inflammation because they comprise macrophage and fibroblast infiltration with collagen deposition, vascularization, and/or epithelial thickening accompanied by a small number of lymphocytes. Accordingly, the four skin-inflammation disorders in which Dsg3 was involved in this study (Table 2) may be categorized as nonspecific inflammatory diseases, although the proportions of cellular and inflammatory components varied. Interestingly, however, these four skin disorders all had mast cell infiltration with degranulation as a common histological feature. In contrast, the scurfy skin disease is a T cell-mediated, chronic delayed hypersensitivity reaction characterized by the presence of epitheloid cells without any mast cell infiltration.

Thus, appearance of anti-Dsg3 and skin inflammation with mast cell infiltration were strongly correlated, although neither the significance of anti-Dsg3 appearance nor mast cell degranulation has been completely addressed here. In addition, the functional relationship between them still remains to be investigated. To address these issues in the future, the establishment of hybridomas producing anti-Dsg3 and the generation of mice lacking only mast cells would be required. Furthermore, the functional relationship of myeloid lineage cells, such as macrophages with mast cells or anti-Dsg3, should be examined. Al-

Table 2. Summary of the relationship between anti-Dsg3 development and histological features

Features	MRL *lpr/lpr*	fsn	me^v/me^v	Scurfy	FcγRIIB $-/-$ immun. with Dsg3
Epidermal thickening	++	+++	−	+	+
Mast cells in the dermis to subcutaneous tissue					
Number	+++	+++	++	−	++
Size	++	++	+	−	++
Degranulation	+	+	+	−	+
Epitheloid cells	−	−	−	++	−
Anti-Dsg3	+++	+	++	+/−	++++

+, Clearly positive; ++, very positive; +++, extremely positive; −, negative; +/−, mostly negative.

though the pathogenic mechanism underlying each skin inflammation studied here may be different, Dsg3 serves as an autoantigen in these chronic skin inflammatory disorders with mast cell infiltration.

Myeloid cells such as macrophages and mast cells are sufficient in the autoinflammatory disorders seen in fsn and me^v mice, with a minimum contribution of anti-Dsg3, whereas, in the immune-complex autoimmune MRL *lpr/lpr* strain, additional appearance of tissue-specific anti-Dsg3, especially anti-Dsg3 IgA, is probably required to enhance malfunction of macrophages and/or mast cells in skin. Considering the fact that antibodies produced in adaptive immunity work synergistically with innate immune components, such as macrophages in a normal immune response, it seems likely that conditions like the skin inflammation in MRL *lpr/lpr* mice may develop in which both innate immune components and antibodies are required to develop diseases. In this sense, immune-complex autoinflammation may be more closely related to autoinflammatory diseases than to autoimmune diseases such as type I diabetes in which tissue-specific T cells greatly contribute.

Dsg3 was originally identified as an autoantigen in the human skin autoimmune disease, bullous PV (18), where separation in the suprabasal layer of the epidermis is present microscopically (27) and leads to deadly macroscopic bulla formation with a minimum of inflammation in the dermis, quite distinct from the skin inflammatory disorders examined here. With immunohistological studies, Ig deposition in intercellular spaces of lower epidermis is present in PV, and sera from PV patients stain normal epidermis. However, neither microscopic splitting (acantholysis) nor Ig deposition in the epidermis has been observed in any of the four skin disorders studied here, despite the presence of anti-Dsg3. In addition, none of the sera from these four skin inflammatory disorders stained epidermis except for nuclei (our unpublished data). Thus, these skin disorders are totally different from human PV histologically and immunohistologically, despite the presence of anti-Dsg3. To explain these different features, the characteristics of anti-Dsg3, e.g., affinity, may be different; anti-Dsg3 with a higher affinity present in human PV may deposit in epidermis by replacing homophilic binding of Dsg3, causing functional blocking of Dsg3, whereas anti-Dsg3 with a lower affinity cannot deposit. Rather, anti-Dsg3 with a lower affinity can bind apoptotic cells expressing Dsg3 from the epidermis and from degenerating lower hair follicles, enhancing scavenger function of macrophage in dermis. The establishment of anti-Dsg3 hybridomas may help elucidate this hypothesis.

The skin inflammations of the murine models studied here have histological pictures that are different from the skin lesions of human SLE (28). However, whether human SLE patients develop anti-Dsg3 or what self-destructive skin inflammatory disorders are human counterparts of these murine models should be further examined to help understand the pathomechanisms of human skin inflammatory disorders.

Materials and Methods

Preparation of Whole-Tissue Extract. Tissues were placed in lysis buffer (420 mM NaCl/250 mM Tris·HCl/5 mM EDTA/1% Triton X-100) including Complete Mini protease inhibitors (Roche, Mannheim, Germany) and homogenized with a polytron. The homogenized tissues were transferred to Eppendorf tubes and incubated on ice for 30 min. After centrifugation at 12,000 × *g* for 15 min, supernatants were collected, and the concentration was measured with Quick Start Bradford dye reagent (Bio-Rad) by determining the absorption at 600 nm.

Preparation of Recombinant Extracellular Domain of Dsg3. Baculoviruses containing extracellular domain of human or mouse Dsg3 (22) were prepared by infecting Sf9 insect cells (Invitrogen) at a multiplicity of infection of one for 5 days and titered with FastPlax titer kit (Novagen) according to the manufacturer's protocol. For the preparation of protein, HiFive insect cells (Invitrogen) were infected with the virus supernatant at a multiplicity of infection of five to 10 for 3 days. The resultant supernatant was collected through a 0.22-μm filter and loaded onto Ni-NTA superflow (Qiagen, Valencia, CA). The beads were washed with washing buffer (50 mM Tris·HCl/500 mM NaCl/40 mM imidazole) and eluted with elution buffer (50 mM Tris·HCl/500 mM NaCl/250 mM Imidazole). The eluant was dialyzed against a solution containing 50 mM Tris·HCl/150 mM NaCl/1 mM EDTA, then concentrated to 1 mg/ml, and stored at −80°C.

Western Blot. Whole-tissue extracts (100 μg with 1% Triton X-100) were subjected to 8% SDS/PAGE and transferred to nitrocellulose membranes (Ready Gel Blotting Sandwiches, Bio-Rad). The membranes were incubated overnight with 5% skim milk in PBS/0.1% Tween 20 at 4°C, then they were incubated with 100× diluted indicated sera. After being washed with PBS/0.1% Tween 20, the membranes were incubated with appropriately diluted horseradish peroxidase (HRP)-conjugated goat anti-mouse IgG (Chemicon International, Temecula, CA). Visualization was done with Western blotting detection reagents (ECL, Amersham Pharmacia Biosciences).

ELISA. Human rDsg at 2.5 μg/ml , anti-mouse Ig at 10 μg/ml (Southern Biotechnology, Birmingham, AL) or DNA from calf thymus at 10 μg/ml (Sigma) were plated at 50 μl per well in 96-well microtiter plates and incubated overnight at 4°C. After being washed three times with 0.05% Tween 20 in Tris-buffered saline (TBS), the plates were incubated with 200 μl of 3% BSA (Sigma) in TBS for 2 h at room temperature. Then the plates were incubated with 100 μl of appropriately diluted serum samples for another 2 h at room temperature. After washing three times with 0.05% Tween 20 in TBS, appropriately diluted goat anti-mouse IgG (Chemicon International) or isotypes (Southern Biotechnology) conjugated with HRP was added and incubated for 1 h. After being washed three times, the plates were developed with an ImmunoPure TMB substrate kit (Pierce) according to the manufacture's protocol, and absorption at 450 nm was measured. As a reference for IgG to Dsg3, HRP-conjugated anti-E Tag (Amersham Pharmacia Biosciences) was used with the value as 100%. For measuring the isotypes, plates were coated with goat anti-Ig then incubated with a series of dilution of each mouse isotype and with respective HRP-conjugated goat anti-mouse isotype (Southern Biotechnology).

Animals. C57BL/6J, BALB/cByJ, A/J, C57BL/6-*lpr/lpr*, C3H-*lpr/lpr*, MRL/MpJ-*lpr/lpr*, C57BL/6-Hcph-me^v (me^v/me^v), Cby.A-fsn/fsn, B6.Cg-Foxp3sf hemizygous male (scurfy), NZB/WF1, NODLt/J, and C57BL/6-FcgRIIB-deficient mice (23) were purchased from The Jackson Laboratory. C57BL/6-FcγRIIB-deficient mice were a gift from Jeffrey Ravetch (The Rockefeller University, New York). Dsg3-deficiecnt mice (21) were from Taconic Farms. Except for scurfy mice, all of the mice used in this paper were female. Sera were collected by retroorbital bleed at the times indicated in Fig. 2. All of the mice were maintained in a specific pathogen-free facility.

Histological and Immunohistological Examination. Tissues were collected in a 4% formaldehyde solution (Sigma), kept for at least one week at 4°C, and then processed by paraffin embedding, sectioning, and standard staining techniques. For mouse CD3 or B220 staining, paraffin-embedded sections were deparaffinized and stained as in F4/80 staining. For F4/80 staining, snap-frozen tissues were embedded in OCT compound (Tis-

sue-Tek, Torrance, CA). Sections measuring 7 μm were fixed with cold acetone and incubated with the antibodies indicated in Fig. 3 after blocking with goat serum. The sections were then incubated with second antibodies conjugated with HRP, developed with diaminobenzidine, and counterstained with hematoxylin.

Immunization. Human rDsg3 or NP-CGG (100 μg for each) (Bioresearch Technology, Novato, CA) in 100 μl of PBS was mixed well with an equal volume of incomplete Freund's adjuvant (Sigma) containing *Mycobacterium tuberculosis* H37 RA (Difco) at a final concentration of 2 mg/ml and injected into mice i.p. The same amount of the proteins in incomplete Freund's adjuvant was injected at 4-week intervals twice.

We thank Drs. Hui-Juan Lv and Lily Tung for support and Drs. Hisashi Umemori, Fukumi Furukawa, John Stanley, and Masayuki Amagai for critical discussion. This study was supported by National Institutes of Health Grant A149554 (to J.L.S.) and by a Human Frontiers of Science Program Fellowship (to H.N.).

1. Vyse, T. J. & Kotzin, B. L. (1998) *Annu. Rev. Immunol.* **16,** 261–292.
2. Furukawa, F., Tanaka, H., Sekita, K., Nakamura, T., Horiguchi, Y. & Hamashima, Y. (1984) *Arch. Dermatol. Res.* **276,** 186–194.
3. Blatt, N. B. & Glick, G. D. (1999) *Pharmacol. Ther.* **83,** 125–139.
4. Cohen, P. L. & Eisenberg, R. A. (1991) *Annu. Rev. Immunol.* **9,** 243–269.
5. Drake, C. G., Rozzo, S. J., Vyse, T. J., Palmer, E. & Kotzin, B. L. (1995) *Immunol. Rev.* **144,** 51–74.
6. Izui, S., Iwamoto, M., Fossati, L., Merino, R., Takahashi, S. & Ibnou-Zekri, N. (1995) *Immunol. Rev.* **144,** 137–156.
7. Chan, O. T., Madaio, M. P. & Shlomchik, M. J. (1999) *Immunol. Rev.* **169,** 107–121.
8. Miwa, T., Maldonado, M. A., Zhou, L., Sun, X., Luo, H. Y., Cai, D., Werth, V. P., Madaio, M. P., Eisenberg, R. A. & Song, W. C. (2002) *Am. J. Pathol.* **161,** 1077–1086.
9. Furukawa, F. & Hamashima, Y. (1982) *J. Dermatol.* **9,** 467–471.
10. Beutler, B. (2004) *Nature* **430,** 257–263.
11. Stojanov, S. & Kastner, D. L. (2005) *Curr. Opin. Rheumatol.* **17,** 586–599.
12. Carroll, M. C. & Holers, V. M. (2005) *Adv. Immunol.* **86,** 137–157.
13. Sundberg, J. P., Beamer, W. G., Shultz, L. D. & Dunstan, R. W. (1990) *J. Invest. Dermatol.* **95,** 62S–63S.
14. Sundberg, J. P., Boggess, D., Sundberg, B. A., Beamer, W. G. & Shultz, L. D. (1993) *Immunol. Invest.* **22,** 389–401.
15. Shultz, L. D., Coman, D. R., Bailey, C. L., Beamer, W. G. & Sidman, C. L. (1984) *Am. J. Pathol.* **116,** 179–192.
16. Sundberg, J. P., Boggess, D., Shultz, L. D. & Beamer, W. G. (1994) in *Handbook of Mouse Mutations with Skin and Hair Abnormalities*, ed. Sundberg, J. P. (CRC, Ann Arbor, MI), pp. 253–268.
17. Yu, C. C., Tsui, H. W., Ngan, B. Y., Shulman, M. J., Wu, G. E. & Tsui, F. W. (1996) *J. Exp. Med.* **183,** 371–380.
18. Amagai, M., Klaus-Kovtun, V. & Stanley, J. R. (1991) *Cell* **67,** 869–877.
19. Godfrey, V. L., Wilkinson, J. E. & Russell, L. B. (1991) *Am. J. Pathol.* **138,** 1379–1387.
20. Godfrey, V. L., Rouse, B. T. & Wilkinson, J. E. (1994) *Am. J. Pathol.* **145,** 281–286.
21. Koch, P. J., Mahoney, M. G., Ishikawa, H., Pulkkinen, L., Uitto, J., Shultz, L., Murphy, G. F., Whitaker-Menezes, D. & Stanley, J. R. (1997) *J. Cell Biol.* **137,** 1091–1102.
22. Ishii, K., Amagai, M., Hall, R. P., Hashimoto, T., Takayanagi, A., Gamou, S., Shimizu, N. & Nishikawa, T. (1997) *J. Immunol.* **159,** 2010–2017.
23. Takai, T., Ono, M., Hikida, M., Ohmori, H. & Ravetch, J. V. (1996) *Nature* **379,** 346–349.
24. Bolland, S. & Ravetch, J. V. (2000) *Immunity* **13,** 277–285.
25. Yuasa, T., Kubo, S., Yoshino, T., Ujike, A., Matsumura, K., Ono, M., Ravetch, J. V. & Takai, T. (1999) *J. Exp. Med.* **189,** 187–194.
26. Nakamura, A., Yuasa, T., Ujike, A., Ono, M., Nukiwa, T., Ravetch, J. V. & Takai, T. (2000) *J. Exp. Med.* **191,** 899–906.
27. Wu, H., Schapiro, B. & Harrist, T. J. (2005) in *Lever's Histopathology of the Skin*, eds. Elder, D. E., Elenitsas, R., Johnson, G. L. J. & Murphy, G. F. (Lippincott, Philadelphia), pp. 253–261.
28. Jaworsky, C. (2005) in *Lever's Histopathology of the Skin*, eds. Elder, D. E., Elenitsas, R., Johnson, G. L. J. & Murphy, G. F. (Lippincott, Philadelphia), pp. 293–306.